

## Competing pinning mechanisms in $\text{Bi}_2\text{Sr}_2\text{CaCu}_2\text{O}_y$ single crystals by magnetic and defect structural studies

G. Yang

*Superconductivity Research Group, The University of Birmingham, Birmingham B15 2TT, United Kingdom*

P. Shang

*Superconductivity Research Group and School of Metallurgy and Materials, The University of Birmingham, Birmingham B15 2TT, United Kingdom*

S. D. Sutton

*Superconductivity Research Group, The University of Birmingham, Birmingham B15 2TT, United Kingdom*

I. P. Jones

*Superconductivity Research Group and School of Metallurgy and Materials, The University of Birmingham, Birmingham B15 2TT, United Kingdom*

J. S. Abell and C. E. Gough

*Superconductivity Research Group, The University of Birmingham, Birmingham B15 2TT, United Kingdom*

(Received 25 March 1993)

A correlation between magnetic hysteresis [measured with a vibrating-sample magnetometer (VSM)] and defect structures (studied by transmission-electron microscopy) is reported for a number of  $\text{Bi}_2\text{Sr}_2\text{CaCu}_2\text{O}_y$  single crystals in the as-grown state and after annealing in oxygen or vacuum above  $400^\circ\text{C}$ . Different regimes of flux pinning can be distinguished from VSM measurements, which we associated with point defects (oxygen vacancies) and planar dislocation networks. Dislocation networks observed in  $\text{Bi}_2\text{Sr}_2\text{CaCu}_2\text{O}_y$  single crystals provide effective pinning centers for decoupled two-dimensional (2D) pancake vortices, especially when the characteristic length scale of the network matches that of the 2D pancake vortex spacing. Anomalies in the magnetic properties are discussed in terms of the competition between pinning from point defects and dislocation networks, together with a transition from a 3D flux lattice to a 2D pancake vortex regime.

High- $T_c$  superconductors possess layered structures and are therefore highly anisotropic. Such anisotropy is conveniently expressed as the ratio  $\Gamma = m_3/m_1$ , where  $m_1$  and  $m_3$  are the effective masses of the quasiparticles for motion parallel and perpendicular to the  $\text{CuO}_2$  planes. For  $\text{Bi}_2\text{Sr}_2\text{CaCu}_2\text{O}_y$ , this value is believed to be in excess of 3000.<sup>1</sup> Such large anisotropy and small coherence length compared with the interlayer spacing results in quasi-two-dimensional superconducting behavior in  $\text{Bi}_2\text{Sr}_2\text{CaCu}_2\text{O}_y$ , just below  $T_c$ .<sup>2</sup> For highly anisotropic layered superconductors, vortex lines can be regarded as two-dimensional (2D) pancake vortices confined to the  $\text{CuO}_2$  layers but weakly interacting between layers by Josephson and magnetic coupling. At low temperature, such coupling results in essentially (3D) flux lines. However, a decoupling transition from 3D flux lattice to 2D pancake vortices will take place at high temperatures and high fields, when the thermal fluctuation energy becomes comparable with the Josephson and magnetic coupling energies between vortices in the different  $\text{CuO}_2$  layers.<sup>3</sup> It is believed that such a decoupling transition occurs in  $\text{Bi}_2\text{Sr}_2\text{CaCu}_2\text{O}_y$  crystals at around 30 K (Ref. 4) but little is known about the pinning of the decoupled pancake vortices in the 2D regime.

Flux pinning in the superconducting state is of importance from the point of view of both theory and potential applications. In high- $T_c$  superconductors, there is little doubt that oxygen vacancies are effective flux-pinning centers<sup>4</sup> and that spatial variation of the oxygen ordering may well account for the anomalous "fishtail" magnetization feature in  $\text{YBa}_2\text{Cu}_3\text{O}_{7-8}$  crystals.<sup>5</sup> A flux line can be pinned along its length by point defects. However, such defects are less effective in pinning 2D pancake vortices, since the pinning energy within a  $\text{CuO}_2$  layer is relatively small. In contrast, extended defects in the basal plane, such as dislocation networks, are likely to be particularly effective in pinning 2D pancake vortices. Dislocation networks will be more effective pinning centers when their length scale matches that of the 2D pancake vortex spacing.<sup>6</sup>

In this paper we present results from magnetic hysteresis measurements and defect structural studies for  $\text{Bi}_2\text{Sr}_2\text{CaCu}_2\text{O}_y$  single crystals both before and after oxygen and vacuum annealing above  $400^\circ\text{C}$ . These results suggest the importance of two pinning mechanisms: oxygen vacancies and dislocation networks. We propose that the observed processing-dependent anomalous magnetization results from a competition between these two pin-

ning mechanisms. Their relative importance reverses above and below the decoupling transition from the 3D flux lattice to 2D pancake vortices confined to the  $\text{CuO}_2$  layers.

$\text{Bi}_2\text{Sr}_2\text{CaCu}_2\text{O}_y$  single crystals were grown using a large temperature gradient technique<sup>7</sup> with starting composition  $\text{Bi}_{2.4}\text{Sr}_2\text{CaCu}_2\text{O}_y$  cooled from 950 to 800 °C at 0.5 °C/h. Several good quality single crystals were selected for vibrating-sample-magnetometer (VSM) and transmission-electron-microscopy (TEM) measurements. The transition temperature  $T_c$  of these crystals, determined from magnetic ac susceptibility and superconducting quantum interference device (SQUID) susceptometer measurements, was  $\sim 90$  K.

To investigate the influence of processing on the anomalous magnetization, measurements of  $T_c$  and magnetic hysteresis over a wide range of temperatures were made before and after annealing the crystals in either oxygen or high vacuum. VSM measurements were performed in a magnetic field parallel to the  $c$  direction at a sweep rate of 1 mT/s using an Oxford VSM 3001. Room-temperature TEM measurements were made using a Philips CM20 mi-

croscope operating at 200 kV and a JEOL 4000 FX for measurements at high temperatures.

A selected crystal (sample 1) of volume  $3.5 \times 2.0 \times 0.01$  mm<sup>3</sup> was annealed at 420 °C in 13.6 bar oxygen pressure for 24 h. After such annealing  $T_c$  decreased from 90 to 86 K but the transition remained sharp with no evidence for any phase separation. In Figs. 1(a)–1(d) we superimpose hysteresis loops for this crystal at representative temperatures measured before and after oxygen annealing. An anomalous peak in the magnetization curves occurs at field of 60–100 mT, as is clearly evident in both sets of measurements. This anomaly appears between 20 and 40 K for the as-grown crystal and between 15 and 45 K after oxygen annealing. The field at which the maximum occurs is almost independent of temperature in both cases although it is increased from about 60 to 100 mT after oxygen annealing. This is very different from the anomalous fishtail magnetization in  $\text{YBa}_2\text{Cu}_3\text{O}_{7-\delta}$  crystals,<sup>8</sup> where the field at which the anomaly occurs decreases with increasing temperature. This suggests that the anomaly in  $\text{Bi}_2\text{Sr}_2\text{CaCu}_2\text{O}_y$  has a different origin from that in  $\text{YBa}_2\text{Cu}_3\text{O}_{7-\delta}$ .

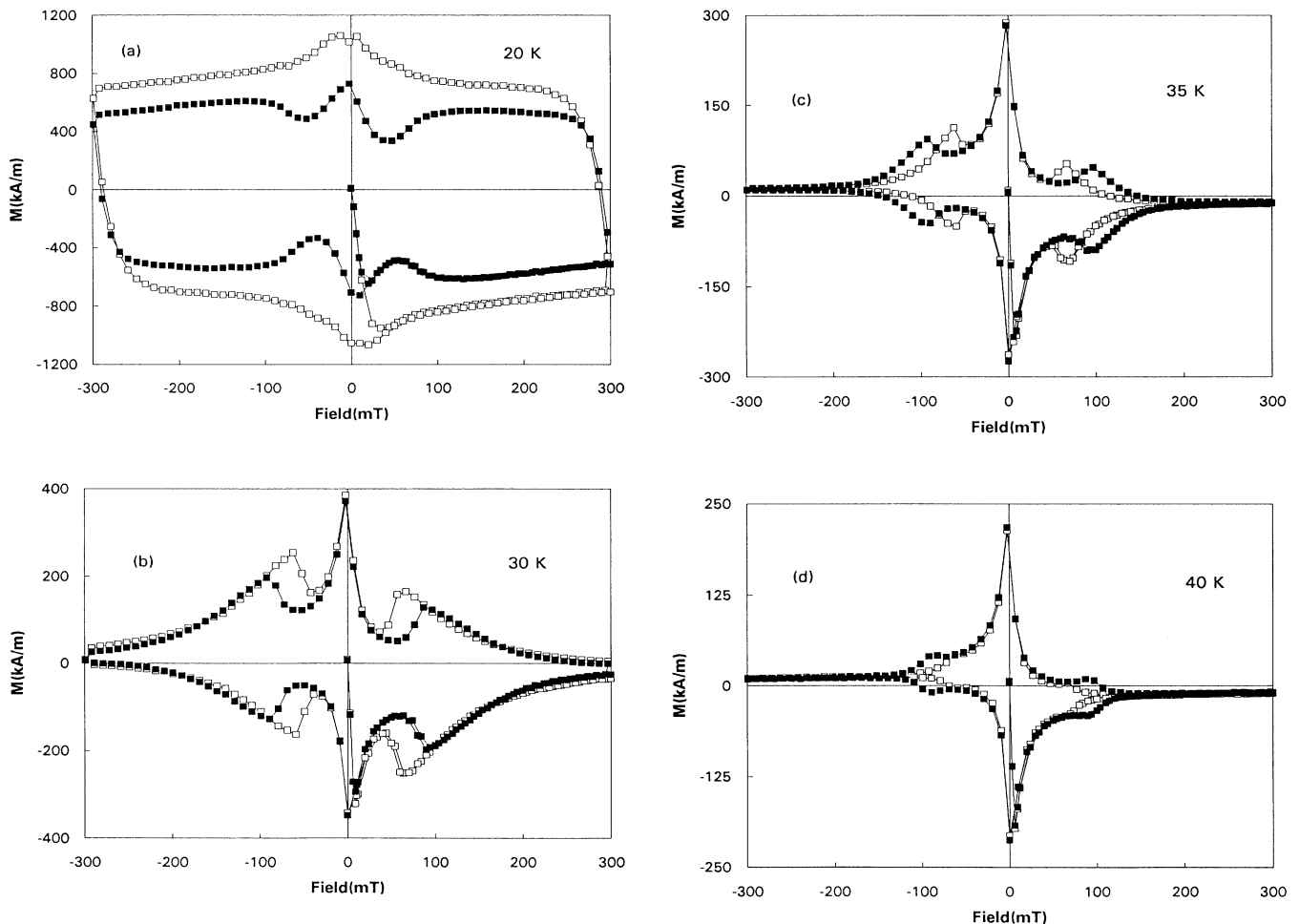


FIG. 1. (a)–(d) Temperature dependence of VSM hysteresis loops for a  $\text{Bi}_2\text{Sr}_2\text{CaCu}_2\text{O}_y$  single crystal (sample 1) before (empty squares) and after (filled squares) oxygen annealing at 420 °C.

Below 25 K the width of the hysteresis loop is decreased after oxygen annealing, suggesting a reduced pinning, consistent with a reduction in the number of point defects (oxygen vacancies). It is interesting to note that above 30 K, the central region of the magnetization curve is almost unchanged after annealing in oxygen. Although the amplitude of the finite field anomaly remains almost constant, it moves to higher fields.

The above behavior should be contrasted with the dependence of the magnetization on vacuum annealing. For such measurements, a second crystal (sample 2) of volume  $2.0 \times 2.0 \times 0.01 \text{ mm}^3$ , was selected and initially annealed in  $6 \times 10^{-6}$  mbar in a vacuum furnace at a relatively low temperature (200 °C) for 25 h. No evidence for any change in  $T_c$  or magnetic properties was found after annealing at this temperature. However, significant changes were observed after annealing at 420 °C at  $2 \times 10^{-5}$  mbar for 25 h. The  $T_c$  decreased from 90 to 87 K and the anomalous magnetization disappeared completely, as illustrated in Figs. 2(a)–2(d). These results suggest that vacuum annealing above 400 °C results in oxygen diffusion out of the crystal, significantly changing the magnetic properties.

In contrast to oxygen annealing, the width of the hysteresis loop below 25 K after vacuum annealing is increased. This is consistent with a model in which oxygen vacancies are assumed to be the major pinning centers at low temperatures. However, in addition to the disappearance of the anomalous magnetization after vacuum annealing, the width of the hysteresis loop above 25 K decreases relative to the as-grown state, which would not be expected if oxygen vacancies alone were the main pinning centers. The above results suggest that oxygen vacancies are the dominant flux-pinning centers at low temperature ( $< 25 \text{ K}$ ) but another pinning mechanism exists above 25 K.

In an attempt to identify the source of such additional pinning, TEM measurements were made on similar crystals from the sample batch. Large scale dislocation networks in the basal  $ab$  plane were observed in about 10% of the specimen areas studied. An example of a highly regular but typical dislocation network image taken by TEM is shown in Fig. 3. A model for such dislocation networks, including identification of Burgers vectors, their geometrical configuration, and formation mechanism, has been presented elsewhere.<sup>9</sup> It is well known

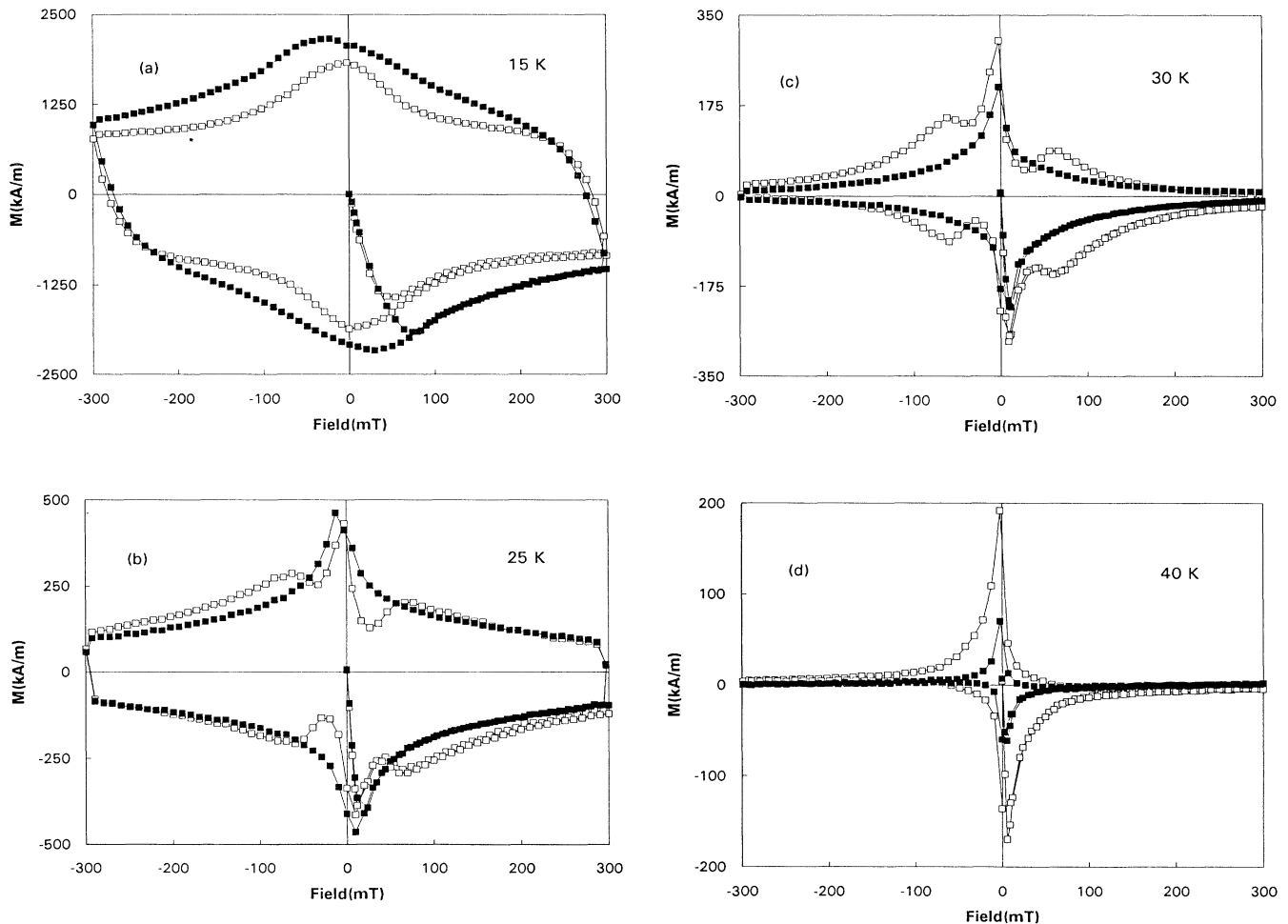


FIG. 2. (a)–(d) Temperature dependence of VSM hysteresis loops for a  $\text{Bi}_2\text{Sr}_2\text{CaCu}_2\text{O}_y$  single crystal (sample 2) before (empty squares) and after (filled squares) vacuum annealing at 420 °C.

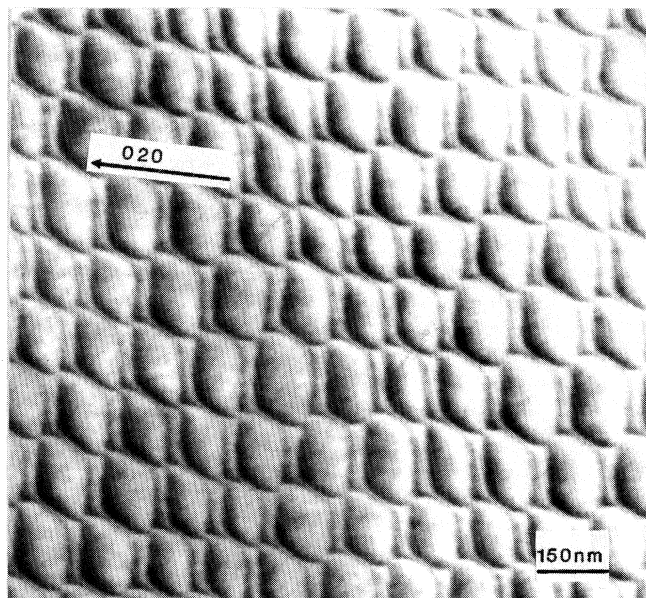


FIG. 3. A TEM image of a highly regular dislocation network of a  $\text{Bi}_2\text{Sr}_2\text{CaCu}_2\text{O}_y$  crystal observed with diffraction vector  $g = [020]$  and near  $[001]$  beam direction.

that dislocation networks can act as effective pinning centers in superconductors.<sup>10–12</sup>

To confirm a correlation between the presence of the dislocation networks and the anomalous magnetization in  $\text{Bi}_2\text{Sr}_2\text{CaCu}_2\text{O}_y$  crystals, we performed an *in situ* TEM study of the effect of temperature annealing on the dislocation networks. Figure 4(a) shows a room-temperature TEM image in an as-grown crystal using a  $g = [020]$  diffraction vector. This micrograph indicates at least two independent planar dislocation networks at different depths within the thinned TEM specimen. Figure 4(b) shows the same region at room temperature after heating the sample for 30 min at  $500^\circ\text{C}$  and then cooling in the microscope. During this period, the electron beam was switched off to avoid possible electron-beam damage at high temperatures. On cooling, the dislocation networks were observed to have almost completely disappeared. At a higher resolution, small regions ( $\sim 10$  nm in size) of a second phase or precipitates are observed, as shown in the inset of Fig. 4(b).

Figures 5(a) and 5(b) show room-temperature diffraction patterns taken before and after vacuum annealing at  $500^\circ\text{C}$  in the microscope. The main structure of the  $\text{Bi}_2\text{Sr}_2\text{CaCu}_2\text{O}_y$  crystal is unchanged but additional broad satellite spots surround the main spots. The additional structure is assumed to rise from the second phase or precipitates. Similar additional diffraction patterns have also been observed by other authors<sup>13</sup> in high-temperature TEM experiments on  $\text{Bi}_2\text{Sr}_2\text{CaCu}_2\text{O}_y$  specimens, although they did not pay attention to the dislocation networks. A sequence of diffraction patterns of a particular region as a function of increasing temperature indicated the new structural feature emerging between 400 and  $465^\circ\text{C}$ . The new structure only appears after

vacuum annealing above  $400^\circ\text{C}$  and is never present in the as-grown crystal. We assume it is associated with oxygen diffusion out of the crystal and the resulting formation of a second phase. The disappearance of the dislocation networks on vacuum annealing above  $400^\circ\text{C}$  has been confirmed over nearly the whole area of three specimens taken from three different single crystals from the sample batch. We therefore believe that this is an intrinsic

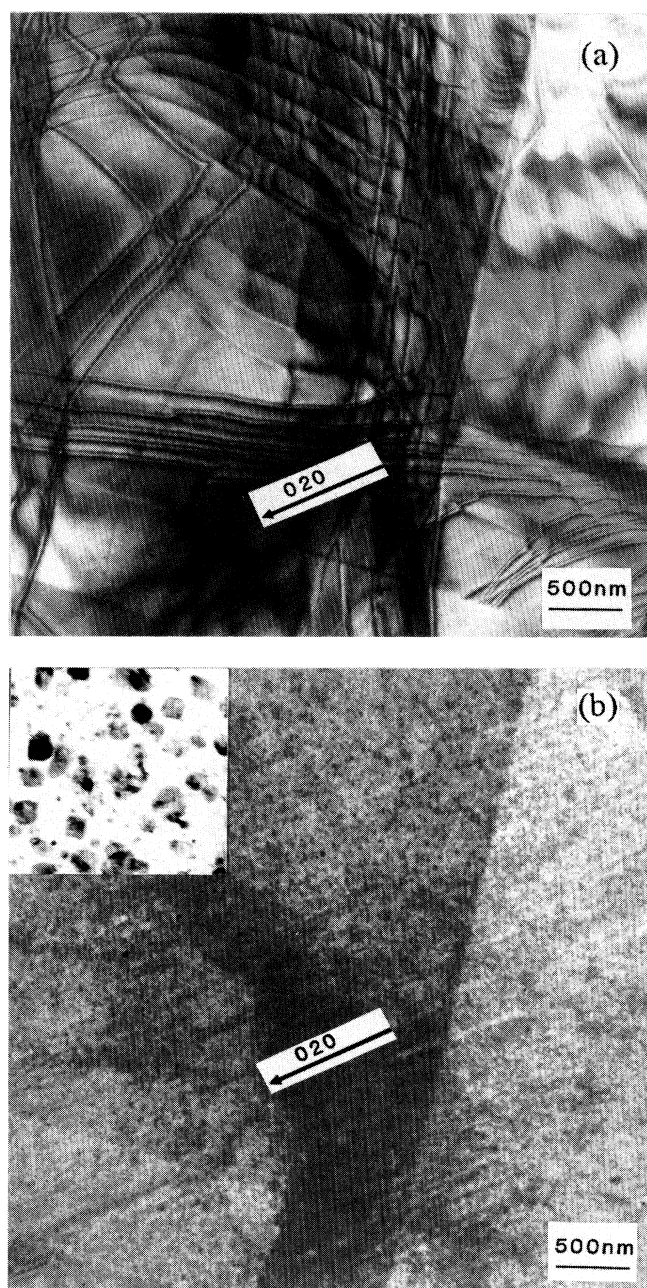


FIG. 4. Room-temperature TEM images of an irregular dislocation network in a  $\text{Bi}_2\text{Sr}_2\text{CaCu}_2\text{O}_y$  crystal (a) before and (b) after heating *in situ* (vacuum) to  $500^\circ\text{C}$  for half an hour. The inset in (b) is at increased magnification showing 10-nm scale precipitates.

sic effect associated with a structural phase transition in vacuum above 400°C.

Annealing specimens in the microscope at  $2 \times 10^{-5}$  mbar is equivalent to the vacuum annealing of sample 2 used for VSM measurements. Similar TEM results were also observed in several specimens cleaved from additional single crystals after annealing in the vacuum furnace. The absence of any anomaly in the magnetic properties of our  $\text{Bi}_2\text{Sr}_2\text{CaCu}_2\text{O}_y$  crystals after vacuum annealing

strongly suggests that the dislocation networks are responsible for the observed magnetic anomaly.

There are a number of experiments which have been interpreted in terms of vortex decoupling transition around 20–30 K in  $\text{Bi}_2\text{Sr}_2\text{CaCu}_2\text{O}_y$  crystals.<sup>14–16</sup> The decoupling transition is marked by a sharp depression of critical current above 25 K. Miller *et al.*<sup>17</sup> proposed that misalignment between pancake vortices in adjacent layers generates a difference in the phase of the order parameter from one layer to the next and that this phase difference locally depresses the critical current density.

Three-dimensional flux lines will be pinned at a number of points in the  $\text{CuO}_2$  layers along their length, so that  $J_c$  will increase with the number of point defects, such as oxygen vacancies. In contrast, the decoupled 2D pancake vortices can only be pinned by such defects in the individual  $\text{CuO}_2$  layers. The energies involved in 2D pinning are relatively small, so that the pancake vortices are more easily depinned by thermal fluctuations, resulting in a rapid decrease in critical current with increasing temperature. Without other effective pinning centers, the decoupled 2D vortex lattice or glassy state will easily melt. However, planar defects, such as the dislocation networks already discussed, are likely to provide strong pinning of the 2D pancake vortices. This will be particularly true when the scale of the dislocation network matches the separation of the pancake vortices.

Figure 6 shows the model for a regular dislocation network typically found in  $\text{Bi}_2\text{Sr}_2\text{CaCu}_2\text{O}_y$  single crystals.<sup>9</sup> The shaded areas are stacking fault regions generated by the dissociation of  $\langle 110 \rangle$  dislocations. As indicated, these stacking fault regions form a triangular lattice with

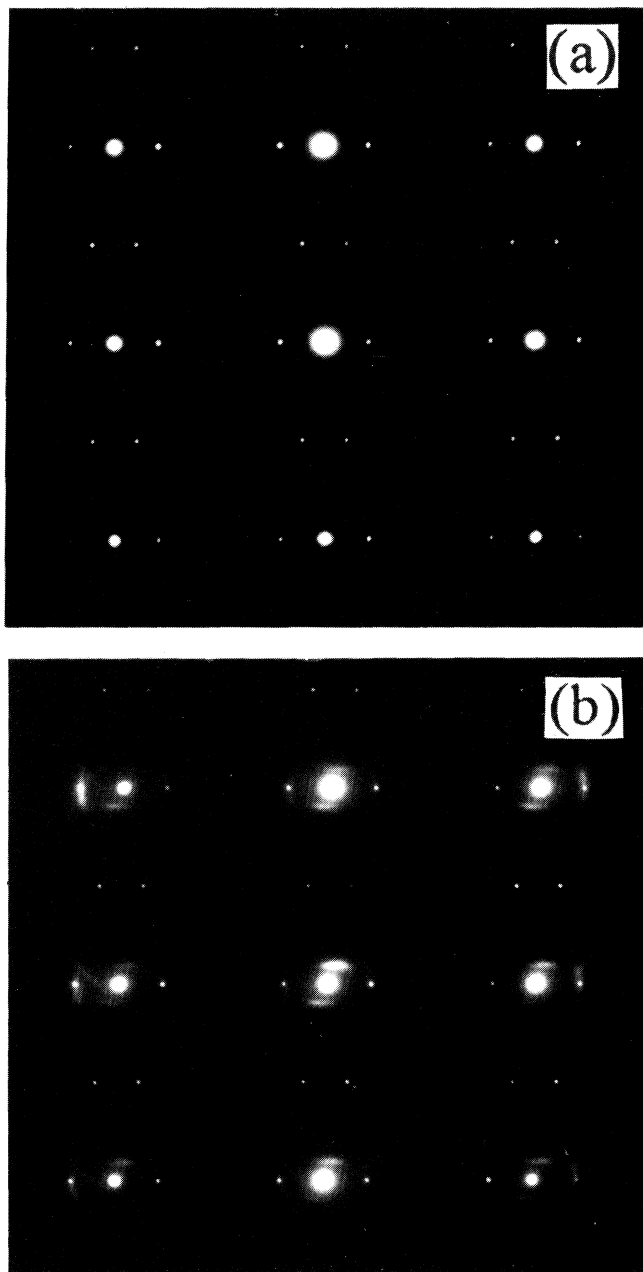


FIG. 5. Room-temperature TEM diffraction patterns with the [001] beam direction from a thinned  $\text{Bi}_2\text{Sr}_2\text{CaCu}_2\text{O}_y$  crystal (a) before and (b) after vacuum annealing in the microscope for half an hour at 500°C.

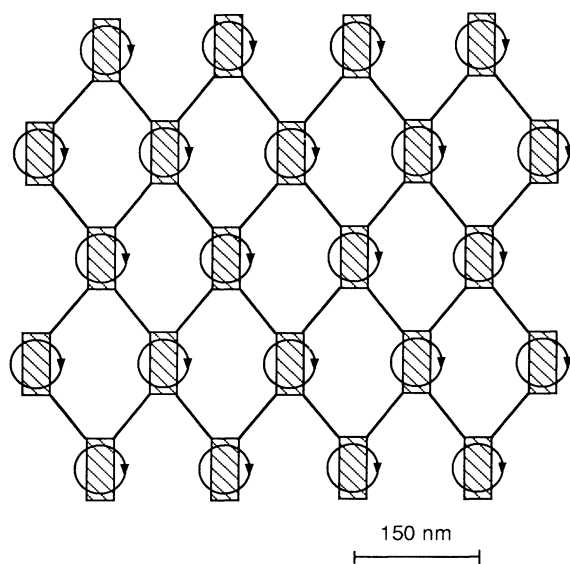


FIG. 6. An idealized dislocation network in the  $\text{Bi}_2\text{Sr}_2\text{CaCu}_2\text{O}_y$  crystal with the shaded areas representing stacking fault regions. The circles represent 2D pancake vortices with a spacing matched to the dislocation network structure.

spacing typically 140 to 200 nm apart. If we assume that pinning is most effective when the spacing of the flux lines matches that of the stacking fault regions, we might expect an enhancement of pinning at around 50 to 100 mT in the magnetic induction, as illustrated schematically in Fig. 6. A similar “matching effect” has been proposed to account for critical-current anomalies in artificially modulated conventional superconductors.<sup>18,19</sup> Figure 7 shows anomalous peak positions of magnetic induction as a function of temperature for the sample 1 crystal before and after oxygen annealing. The lack of any marked temperature dependence of the magnetic induction at which the anomaly occurs in our measurements on  $\text{Bi}_2\text{Sr}_2\text{CaCu}_2\text{O}_y$  crystals is consistent with a spatial matching of the 2D pancake vortices to the scale of the defect structure. Additional support for such a model is derived from the observation that the dislocation networks and the anomalous magnetization both disappear after vacuum annealing above 400 °C.

We also note that the anomalous peak moves to higher  $B$  fields after oxygen annealing. This suggests that the characteristic scale of the network structure is strongly dependent on oxygen stoichiometry. Unfortunately, it has not proved possible to examine the same specimen before and after high-temperature oxygen annealing, as the grid supporting the highly thinned specimen tends to deform at high temperatures in oxygen. On a number of TEM specimens, we do indeed observe a higher density of dislocation networks after high-temperature oxygen annealing. However, given the natural variation in network length scale within a single specimen, the statistics are not sufficient to demonstrate reliably a dependence of dislocation network length scale on oxygenation.

The magnetic interaction of 2D pancakes varies logarithmically with their separation<sup>20</sup> resulting in a long-range correlation of vortices within individual double  $\text{CuO}_2$  layers. Relatively small regions of the dislocation network may therefore be sufficient to pin the 2D vortices over an appreciable area. However, the matching of a 3D flux lattice to such dislocation networks can only take place within a single plane, as there is no correlation between the dislocation networks on different planes. We would not expect matching to be effective along the length of a straight 3D flux-line lattice. Such networks would therefore not be expected to be the dominant pinning mechanism for the 3D flux lattice at low temperatures.

No anomalies were observed at fields corresponding to a flux vortex spacing that was a multiple or submultiple of the dislocation network length scale. Matching at lower fields may be inhibited because vortices remain 3D and may not have decoupled between layers. At high fields, the anomaly will be broadened by the natural variations in the dislocation network length scale.

Based on the above observations, we believe that there exist two principal flux-pinning mechanisms in our  $\text{Bi}_2\text{Sr}_2\text{CaCu}_2\text{O}_y$  crystals. Below 25 K, oxygen vacancies are likely to be the dominant source of pinning for the 3D flux lattice, with planar dislocation networks playing a

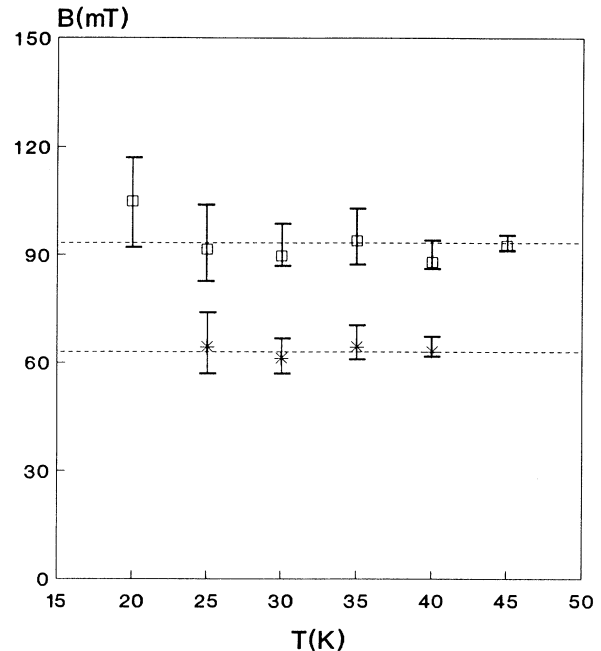


FIG. 7.  $B$  field at anomaly peak position as a function of temperature for sample 1 crystal before (stars) and after (squares) oxygen annealing.

secondary role. Above 25 K, the pancake vortices undergo a 3D to 2D transition. Spatial matching of the decoupled 2D pancake vortices to the dislocation networks are then assumed to be responsible for the anomalous peak observed in the magnetization at around 60–100 mT. Above 40 K, thermal fluctuation energies are sufficient to overcome both kinds of pinning and the magnetization becomes nearly reversible.

In summary, magnetic hysteresis and defect structural studies on  $\text{Bi}_2\text{Sr}_2\text{CaCu}_2\text{O}_y$  single crystals as a function of annealing in oxygen and vacuum suggest the existence of two principle pinning mechanisms for magnetic flux. At low temperature, the dominant pinning depends on the degree of sample oxygenation and is almost certainly due to point defects (oxygen vacancies) pinning the 3D flux lattice. On raising the temperature above 25 K, thermal fluctuation results in a vortex structure transition from 3D to 2D pancake vortices on the individual  $\text{CuO}_2$  layers with little correlation between layers. Decoupled 2D pancake vortices interact strongly with the extended dislocation networks observed in the specimens by TEM. This pinning is expected to be particularly strong when the pancake vortex spacing matches that of the network structure leading to the pronounced peak observed in the magnetic hysteresis at around 60–100 mT. The temperature and field dependence of the magnetic hysteresis can be understood in terms of a competition in pinning from point defects and the dislocation networks, which reverse their relative importance above and below the 3D to 2D transition at around 25 K.

- <sup>1</sup>D. E. Farrell, S. Bonham, J. Foster, Y. C. Chang, P. Z. Jiang, K. G. Vandervoort, D. J. Lam, and V. C. Kogan, *Phys. Rev. Lett.* **63**, 782 (1989).
- <sup>2</sup>P. H. Kes, J. Aarts, V. M. Vinokur, and C. J. van der Beek, *Phys. Rev. Lett.* **64**, 1063 (1990).
- <sup>3</sup>J. R. Clem, *Phys. Rev. B* **43**, 7837 (1991).
- <sup>4</sup>P. H. Kes, in *Phenomenology And Applications On High-Temperature Superconductors*, edited by K. Bedell *et al.* (Addison-Wesley, New York, 1992), p. 390.
- <sup>5</sup>Joao L. Vargas and David C. Larbalestier, *Appl. Phys. Lett.* **60**, 1741 (1992).
- <sup>6</sup>G. Yang, C. E. Gough, and J. S. Abell, *IEEE Trans. Appl. Supercond.* (to be published).
- <sup>7</sup>G. Yang, S. D. Sutton, P. Shang, C. E. Gough, and J. S. Abell, *IEEE Trans. Appl. Supercond.* (to be published).
- <sup>8</sup>C. E. Gough, G. Yang, M. Z. Shoushtari, T. G. N. Babu, F. Gencer, and J. S. Abell, *Physica C* **185-189**, 2359 (1991).
- <sup>9</sup>P. Shang, G. Yang, I. P. Jones, C. E. Gough, and J. S. Abell, *Appl. Phys. Lett.* (to be published).
- <sup>10</sup>A. V. Narlikar and D. Dew-Hughes, *Phys. Status Solidi* **6**, 383 (1964).
- <sup>11</sup>E. J. Kramer, *Philos. Mag.* **33**, 331 (1976).
- <sup>12</sup>C. S. Panda, *Appl. Phys. Lett.* **28**, 462 (1976).
- <sup>13</sup>C. Chen, J. W. Li, Y. S. Yao, X. M. Huang, Z. X. Zhao, and W. K. Wang, *Solid State Commun.* **68**, 749 (1988).
- <sup>14</sup>C. Duran, J. Yazzi, F. de la Cruz, D. J. Bishop, D. B. Mitzi, and A. Kapitulnik, *Phys. Rev. B* **44**, 7737 (1991).
- <sup>15</sup>D. H. Kim, K. E. Gray, R. T. Kampwirth, J. C. Smith, D. S. Richeson, T. J. Marks, J. H. Kang, J. Talvacchio, and M. Eddy, *Phys. C* **177**, 431 (1991).
- <sup>16</sup>H. Safar, P. L. Gammel, D. J. Bishop, D. B. Mitzi, and A. Kapitulnik, *Phys. Rev. Lett.* **68**, 2672 (1992).
- <sup>17</sup>S. L. Miller, K. R. Biagi, J. R. Clem, and D. K. Finnemore, *Phys. Rev. B* **31**, 2684 (1985).
- <sup>18</sup>H. Roffy, E. Guyon, and J. C. Renard, *Solid State Commun.* **14**, 427 (1974); **14**, 431 (1974).
- <sup>19</sup>O. Daldini, P. Martinoli, and J. L. Olsen, *Phys. Rev. Lett.* **32**, 218 (1974).
- <sup>20</sup>J. Pearl, *Appl. Phys. Lett.* **5**, 65 (1964).

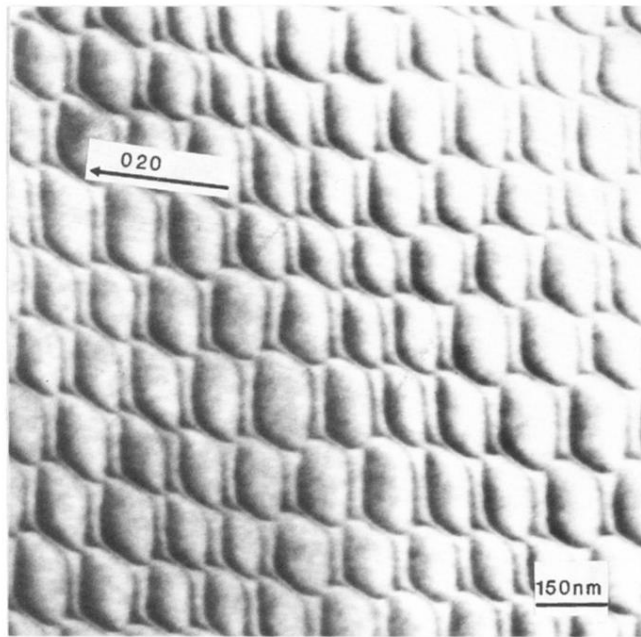


FIG. 3. A TEM image of a highly regular dislocation network of a  $\text{Bi}_2\text{Sr}_2\text{CaCu}_2\text{O}_y$  crystal observed with diffraction vector  $g = [020]$  and near  $[001]$  beam direction.



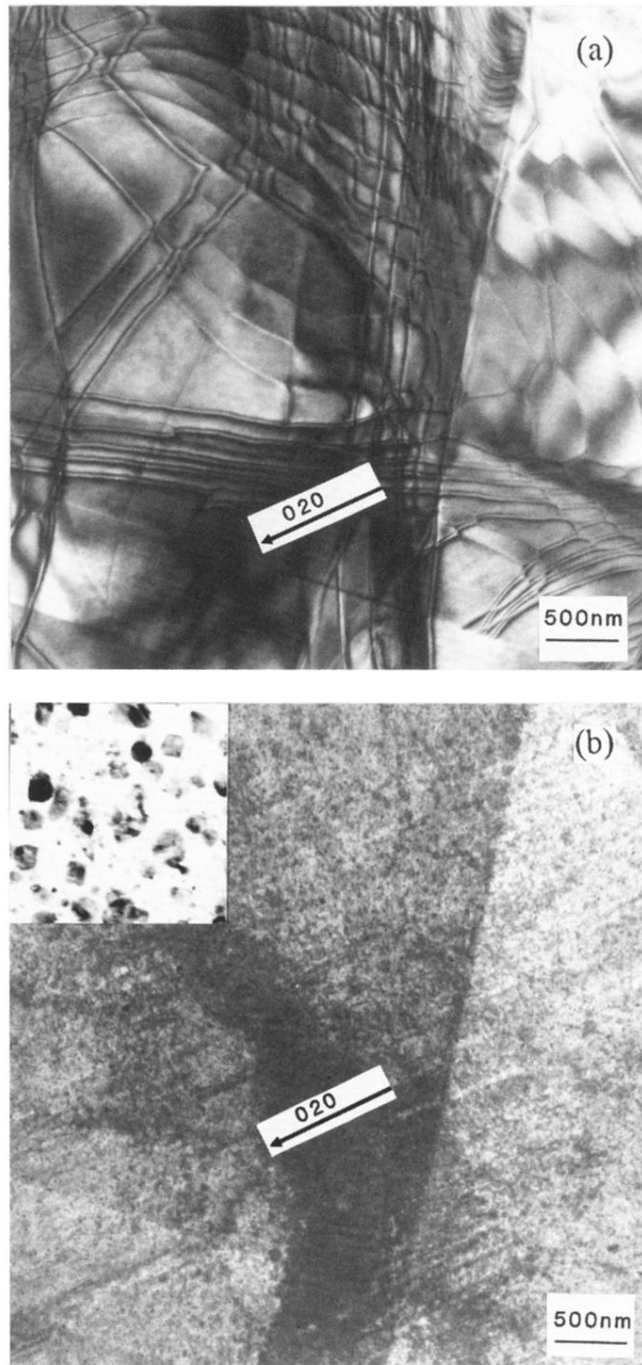


FIG. 4. Room-temperature TEM images of an irregular dislocation network in a  $\text{Bi}_2\text{Sr}_2\text{CaCu}_2\text{O}_y$  crystal (a) before and (b) after heating *in situ* (vacuum) to 500 °C for half an hour. The inset in (b) is at increased magnification showing 10-nm scale precipitates.

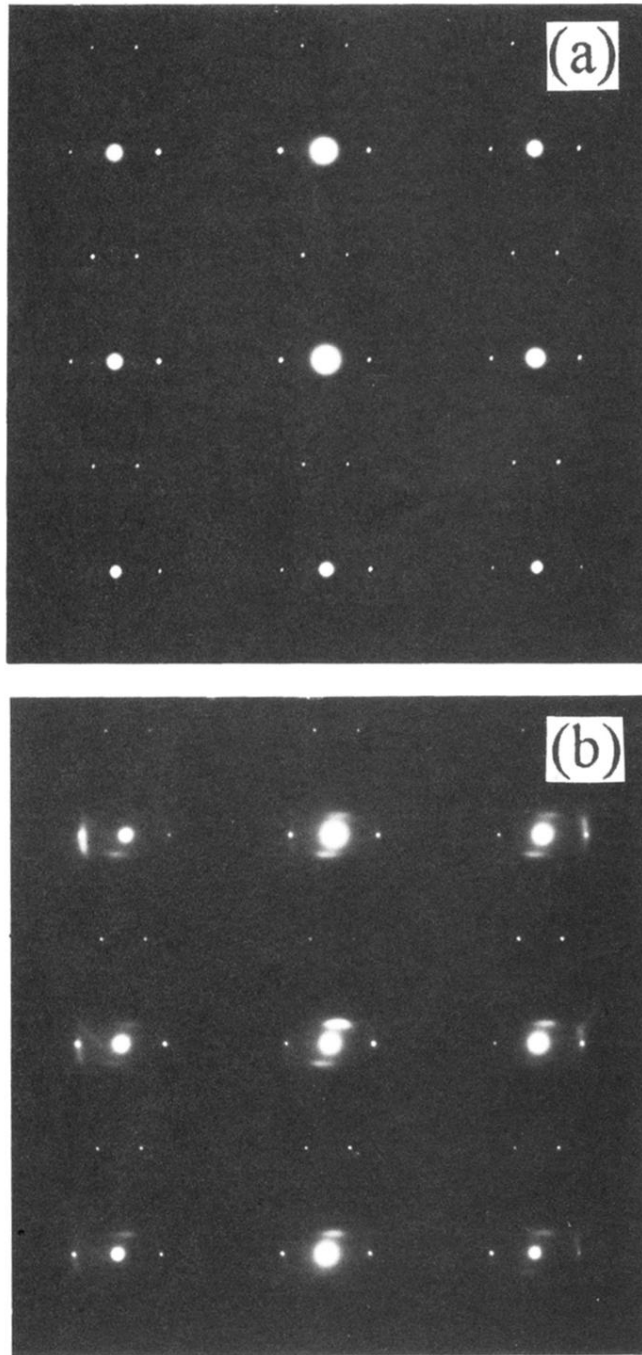


FIG. 5. Room-temperature TEM diffraction patterns with the [001] beam direction from a thinned  $\text{Bi}_2\text{Sr}_2\text{CaCu}_2\text{O}_y$  crystal (a) before and (b) after vacuum annealing in the microscope for half an hour at 500°C.